ACTA NEUROBIOLOGIAE EXPERIMENTALIS

Research Paper Acta Neurobiol Exp 2013, 73: 143–156

Epigenetic and molecular signature of human umbilical cord blood-derived neural stem cell (HUCB-NSC) neuronal differentiation

Aleksandra Habich [1,2], Ilona Szablowska-Gadomska[1], Valery Zayat[1], Leonora Buzanska[1], and Krystyna Domańska-Janik[1]*

[1]NeuroRepair Department, Mossakowski Medical Research Centre, Polish Academy of Sciences, Warsaw, Poland, *Email: krystyna.dj@gmail.com; [2]Stem Cell Laboratory, Department of Neurology and Neurosurgery, Faculty of Medical Sciences, University of Warmia and Mazury, Olsztyn, Poland

In the context of cell therapy, the epigenetic status of core stemness transcription factor (STF) genes regulating the cell proliferation/differentiation program is of primary interest. Our results confirmed that *in vitro* differentiation of the umbilical-cord-blood-derived-neural-stem-cells (HUCB-NSC) coincides with the progressive down-regulation of Oct3/4 and Nanog gene expression. Consistently and in parallel with the repression of gene transcription, a substantial increase in the mosaic cytosine methylation CpG dinucleotide was observed in the promoter regions of these STF genes. However none of the histone-H3 post-translational-modifications (PTM) known to be associated with transcriptionally active genes (H3Ac and H3K4me3) or repressed genes (H3K9me3 and H3K27me3) seemed to vary in relation to the progression of cell differentiation and down-regulation of STF genes. This indicates an uncoupling between STF gene expression and above mentioned histone PTMs. In contrast, the overall methylation of nuclear chromatin at repressive histone H3K9me3 was significantly higher than H3K4 trimetylation in expanding HUCB-NSC cultures and then increases through the progression of cell differentiation. These observations suggest different epigenetic programs of gene repression realized in the cell nuclei of differentiating HUCB-NSC cultures with uneven involvement of the repressive histone PTMs.

Key words: neural stem cells, umbilical cord blood, epigenetic changes

INTRODUCTION

Neural stem cells (NSCs) are multipotent progenitors with promising therapeutic applications in various neurodegenerative and acute CNS diseases. These cells are relatively rare among the other neural cells (Reynolds and Rietze 2005) and they do not respond adequately to the regenerative needs of injured nervous tissue. They are also situated in distinct intra-cerebral regions which restrict their access, thereby reducing the success of isolating adequate numbers needed for cell-replacement therapy. Consequently, for more than decade, our group (Buzanska et al. 2002, Habich et al. 2006, Jurga et al. 2009) as well as others (Sanchez-Ramos et al. 2001, Kogler et al. 2004, McGuckin et al. 2004, Lee et al. 2007, Ali et al. 2009, Chua et al. 2009), have worked on cord blood (CB) as an alternative source of readily accessible therapeutically competent (Zigova et al. 2002, Willing et al. 2003) stem cells with an intrinsic potential for neural differentiation.

Broadening the scope of cord blood cells utilized for neurological therapies remains a major challenge as it is dependent on the understanding of the control mechanism(s) that underlie their flexibility toward attaining a pro-neural phenotype. This transition of the cell fate may mainly rely on the extensive epigenetic remodeling induced by the influence of various environmental factors and genetic manipulations. As a result, the cell transcriptional activity would be reprogrammed due to induced changes in the expression of key regulatory genes which, depending on their nature, would be activated or silenced during neural cell differentiation.

Correspondence should be addressed to K. Domańska-Janik Email: krystyna.dj@gmail.com

Received 06 November 2012, accepted 26 February 2013

Recent findings suggest that the transduction of certain genes (constitutive or transient) that lead to the expression of only a few "stemness" transcription factors (STF), such as Oct3/4, or Sox2 (Yamanaka 2007) which, together with Nanog (being previously reported to be activated in pluripotent stem cells), induce an embryonic stem cell-like behavior in matured cells. More recently, human umbilical cord blood was demonstrated to respond to this type of induced pluripotency (iPS) (Haase et al. 2009, Zaehres et al. 2010, Giorgetti et al. 2010). On the other hand, there is also an increasing body of evidence that suggests an almost unlimited plastic potential of primitive, embryonic-like progenitors, present in the cord blood. These cells would be responsible for redirection of cell differentiation and spontaneous lineage switching *in vitro* and *in vivo* (Bonner-Weir et al. 2008, Borowiak and Melton 2009, Vierbuchen et al. 2010).

It is still unclear whether the exposure of such specific stimuli would induce the cells to disregard their actual phenotypic identity due to epigenetic reprogramming through mechanisms described as trans- or dedifferentiation or whether they acquire these new features by rapid expansion and differentiation of the preexisting, small, embryonic-like subpopulation (McGuckin et al. 2005, Habich et al. 2006, Kucia et al. 2007) being positively selected under the influence of the changed environment.

In spite of these unresolved questions, the defined cell lineage development would involve specific epigenetic post- translational modifications (PTMs), controlling step transition of the most primitive cells up to matured phenotypes of their terminal differentiation.

In the present study, we exploit the CB-derived untransformed cell line with molecular and functional neural stem cell characteristic named HUCB-NSC developed in our laboratory (Sun et al. 2005, Buzanska et al. 2006, 2009). We have critically evaluated the interdependency between the defined stages of neuronal differentiation, the transcriptional activity of core STF genes Oct3/4, Nanog, and defined epigenetic modifications. This latter included a dissection of the chromatin modification on the level of DNA methylation and histone acetylation and methylation in the promoter regions of Oct3/4 and Nanog genes under influence of a strictly defined neurogenic environment.

The standardized conditions for the lineage-directed and development-dependent stages of neural differentiation of HUCB-NSCs were established in our previous studies by the screening of stage-specific genes and proteins (Buzanska et al. 2006, Domanska-Janik et al. 2008, Jurga et al. 2009). The ability to maintain HUCB-NSC at different developmental levels, starting from pluripotent, non-adherent cell population, through neurally committed but non-differentiated, proliferating precursors up to terminally differentiated cells of neuronal identity, enable us to observe epigenetic correlations with all of these crucial developmental steps. To our knowledge, although mechanistically still unclear, this is the first study directed toward examining the epigenetic shift during human cord blood- derived neural stem cell differentiation.

METHODS

Expansion of HUCB-NSCs in different culture conditions

The NSC line derived from human umbilical cord blood was established and described previously (Buzanska et al. 2006). Approval of a local Ethical Committee and the mother's informed consent was obtained. Cord blood was collected after the delivery of the placenta by puncturing the umbilical cord veins followed by an isolation of mononuclear cell fraction on a Ficoll/Hypaque gradient. The culture of HUCB-NSC was carried out in two different conditions: non serum or low serum conditions as described (Buzanska et al. 2006). Additionally HUCB-NSC were maintained in neuronal differentiating medium containing 2% FBS and supplemented with dBcAMP (100 μM; Sigma). All cultures were maintained at 37°C, 5% CO_2, and 95% humidity.

RNA extraction and PCR analysis

Total RNA was isolated from HUCB-NSC after 14 DIV of culture in serum-free, low serum or cAMP differentiating medium using the RNeasy Mini Kit (Qiagen Inc). A 1 μg of mRNA was reverse transcripted with 200 units of SuperScript Rnase H^- Reverse Transcriptase in its associated buffer, 1 μg of oligo-dT, 400 μM of dNTPs and 40 units of RNase out. cDNA fragments were amplified for 30 cycles (94°C, 2 min; 58°C, 1 min

30 s; 72°C, 2 min) with Taq DNA Polymerase, with 1 μM of forward (F) and reverse (R) primers, respectively. Primer sets for PCR are as follows: Oct3/4 forward, 5'-CTCTGAGGAGTGGGGGATTC-3'; Oct3/4 reverse, 5'-TTGTGCATAGCCACTGCTTG-3'; Nanog forward' 5'-CCTGTGATTTGTGGGCCTG-3'; Nanog reverse, 5'-GACAGTCTCCGTGTGTGAGGCAT-3'; GAPDH forward, 5'-TGAAGGTCGGAGTCAACGGATTTGG-3'; GAPDH reverse, 5'-CATGTAGGCCATGAGGTCCACCAC-3'. PCR products were separated by electrophoresis on 1% agarose gel in 0.5×TBE buffer and visualized by ethidum bromide staining. The gel images were acquired with a GelExpert 4.0.

DNA isolation and bisulfite sequencing

DNA samples were extracted from HUCB-NSCs cultured in serum-free, low serum and cAMP differentiating medium. DNA from hESCs was received from Prof. Dvorak laboratory in Brno. After DNA purification (DNeasy Tissue Kit; Qiagen) bisulfite conversion was performed with the EpiTec Kit (Qiagen) as described by the manufacturer. Fresh or −20°C stored converted DNA was amplified by polymerase chain reaction (PCR) by using primers published by Freberg and colleagues (2007) (primer sequences are listed in Table I). Then PCR reactions were performed under previously established conditions (Freberg et al. 2007) (95°C for 10 min, 40 cycles of 95°C for 1 min, 58°C or 55°C for 1 min and 72°C for 1 min, followed by 10 min at 72°C). PCR products were purified from agarose gel with the Gene MATRIX Agarose-Out DNA Purification Kit (EUREX), and then cloned into pGEM-T Easy Vector System (Promega). Plasmid DNA was isolated using GenElute™ Plasmid Miniprep Kit (Sigma-Aldrich). Sequences of at least 5 bacterial clones per genomic region were examined.

Immunocytochemistry

HUCB-NSC cultured in low serum, serum-free and cAMP differentiation medium were fixed with 4% PF and then blocked with 10% normal goat serum (NGS; Sigma) or 10% albumin from bovine serum (BSA; Sigma) diluted with 0.1% Triton X-100 at room temperature (RT) for 60 minutes. The cells were then incubated with primary antibodies overnight at 4°C: anti-Histone H3 tri methyl K9 (Abcam), anti-Nestin (R&D Systems), anti-GFAP (Cappel), anti-NF200 (Sigma), anti-class III beta-tubulin (Covance) and anti-MAP2 (Sigma). Also proliferating cells were visualized by Ki67 (Novocastra) staining. After washing with PBS cells were exposed to goat anti-mouse IgG1, IgG2b or goat anti-rabbit IgG (HDL) secondary antibodies conjugated with Alexa 488 or Alexa 546 for 60 minutes at RT in the darkness. Additionally cell nuclei were stained with 5 uM Hoechst 33258 for 20 minutes. After final washes the slides were mounted with Fluoromount-G (Southern Biotechnology Association, Birmingham, AL, USA). On parallel slides, staining of cells with omitted primary antibodies served as negative controls. Images were processed using Zeiss LSM 510 software package v. 2.8 and Corel Draw v. 9.0.

Western blotting

Histone proteins were extracted from cell cultures by lysis in Triton Extraction Buffer containing 0.5% Triton X 100 and 2 mM phenylmethylsulfonyl fluoride (PMSF) for 10 minutes on ice, followed by acid extraction overnight. Protein content was evaluated by Lowry assay. The equal volume samples were separated by SDS-PAGE on a 12% polyacrylamide gel and transferred onto Hybon-C-Extra. Immunodetection was performed using the polyclonal anti H3K9me3 and monoclonal anti H3K4me3 antibodies for the samples and polyclonal anti H4 (Abcam) antibody for the common input blot detection. The immunoblots were incubated with horseradish-peroxidase-conjugated secondary antibodies.

Matrix ChIP assay

Chromatin and DNA preparation was done as described previously (Flanagin et al. 2008, Yu et al. 2011). Briefly, cell (10^6 cells) were cross-linked with 1% formaldehyde for 10 min at RT followed with quenching with 125 mM Glycine for 5 min at RT. Cell lysis was performed in IP buffer (150 mM NaCl, 50 mM Tris-HCl (pH 7.5), 5 mM EDTA, 0.5% NP-40, 1% Triton X-100) followed by chromatin shearing in Next-gen Bioruptor (Diagenode) using the protocol 30 s on–off cycles for 15 min at high intensity. The samples were centrifuged at 12 000×g, aliquoted and stored at −80°C. To prepare DNA input, chromatin was incubated with proteinase K (0.2 μg/μl) for 15 minutes at 55°C, followed by 15 minutes at 95°C. Normal rabbit IgG was used as a negative control

Table I

Bisulfite sequencing, ChIP and Real Time PCR primers used in this study		
Gene name	Forward primer (F) Reverse primer (R)	Annealing temp. (°C)
Bisulfite sequencing primers		
OCT3/4 –DE	F: TTAGGAAAATGGGTAGTAGGGATTT	58
	R: TACCCAAAAAACAAATAAATTATAAAACCT	
NANOG1	F: AGAGATAGGAGGGTAAGTTTTTTTT	58
	R: ACTCCCACACAAACTAACTTTTATTC	
NANOG2	F: GAGTTAAAGAGTTTTGTTTTTAAAAATTAT	58
	R: TCCCAAATCTAATAATTTATCATATCTTTC	
NANOG3	F: TTAATTTATTGGGATTATAGGGGTG	55
	R: AACAACAAAACCTAAAAACAAACC	
ChIP primers		
ACTB	F: ACGCCTCCGACCAGTGTT	60
	R: GCCCAGATTGGGGACAAA	
NANOG	F: GTTCTGTTGCTCGGTTTTCT	60
	R: TCCCGTCTACCAGTCTCACC	
OCT3/4	F: GAGGATGGCAAGCTGAGAAA	60
	R: CTCAATCCCCAGGACAGAAC	
RHO	F: TGGGTGGTGTCATCTGGTAA	60
	R: GGATGGAATGGATCAGATGG	
Real-time PCR primers		
GAPDH	F: TCGGAGTCAACGGATTTGGT	60
	R: TTGCCATGGGTGGAATCATA	
OCT3/4	F: GACAGGGGGAGGGGAGGAGCTAGG	60
	R: CTTCCCTCCAACCAGTTGCCCCAAAC	
NANOG	F: CAAAGGCAAACAACCCACTT	60
	R: TCTGCTGGAGGCTGAGGTAT	

Polypropylene plates were incubated overnight with Protein A (0.2 µg) and blocked for 30 min in blocking buffer (5% BSA, 100 µg/ml sheared salmon sperm DNA in IP buffer). The wells were incubated with antibodies (Pol II CTD [Abcam]; H3 [Abcam]; H3Ac [Abcam]; H3K27m3 [Millipore]; H3K9m3 [Abcam]; H3K4m3 [Millipore]) for 1h followed by incubation with chromatin samples in blocking buffer in sonicator bath at 4°C. After washing three and one time with IP and TE buffer, respectively, the DNA was recovered with elution buffer (25 mM Tris, 1 mM EDTA, and 0.2 µg/µl proteinase K) for 15 minutes at 55°C, followed by 15 minutes at 95°C. The samples were stored in −20°C in the same plate for multiple uses.

Reverse Transcription and qPCR analysis

Total RNA was extracted from cells using TRIzolPlus RNA purification kit (Invitrogen) followed by DNA-free™ DNase (Ambion) treatment. One μg of total RNA was used in cDNA synthesis using High Capacity RNA-to-cDNA Master Mix (Invitrogen).

Quantitative evaluation of cDNA and DNA was carried out in a 384-well reaction plate on the ABI 7900HT Real Time PCR system (Applied Biosystems). The reaction mix contained the following components: 2.0 μl 2× SensiMix SYBR Hi-ROX (Bioline), 1.9 μl cDNA/DNA template and 0.1 μl primers (10 μM) in 4 μl final volume. Primers used are listed in Table I. Quantitative RT-PCR reactions were performed in triplicates and expression levels of transcripts were normalized to GAPDH using ΔΔCt method (Pfaffl 2001). ChIP DNA expressions levels were calculated as a fraction of input DNA using the formulas described previously (Flanagin et al. 2008).

Statistical analysis

Statistical analyses were performed using GraphPad Prism (Statistical Software). Statistical significance was assessed by the one-way analysis of variance (ANOVA) in conjunction with Bonferroni's Multiple Comparison Test. Differences were considered statistically significant when P values were lower than 0.05. All data are presented as mean values ± standard deviation.

RESULTS

Stage characteristic of HUCB-NSC line growing under defined culture conditions

The HUCB-NSC culture growing under strictly determined conditions, attained cell phenotypes which mimic defined developmental stages of neural cell differentiation process (Buzanska et al. 2009). In serum-

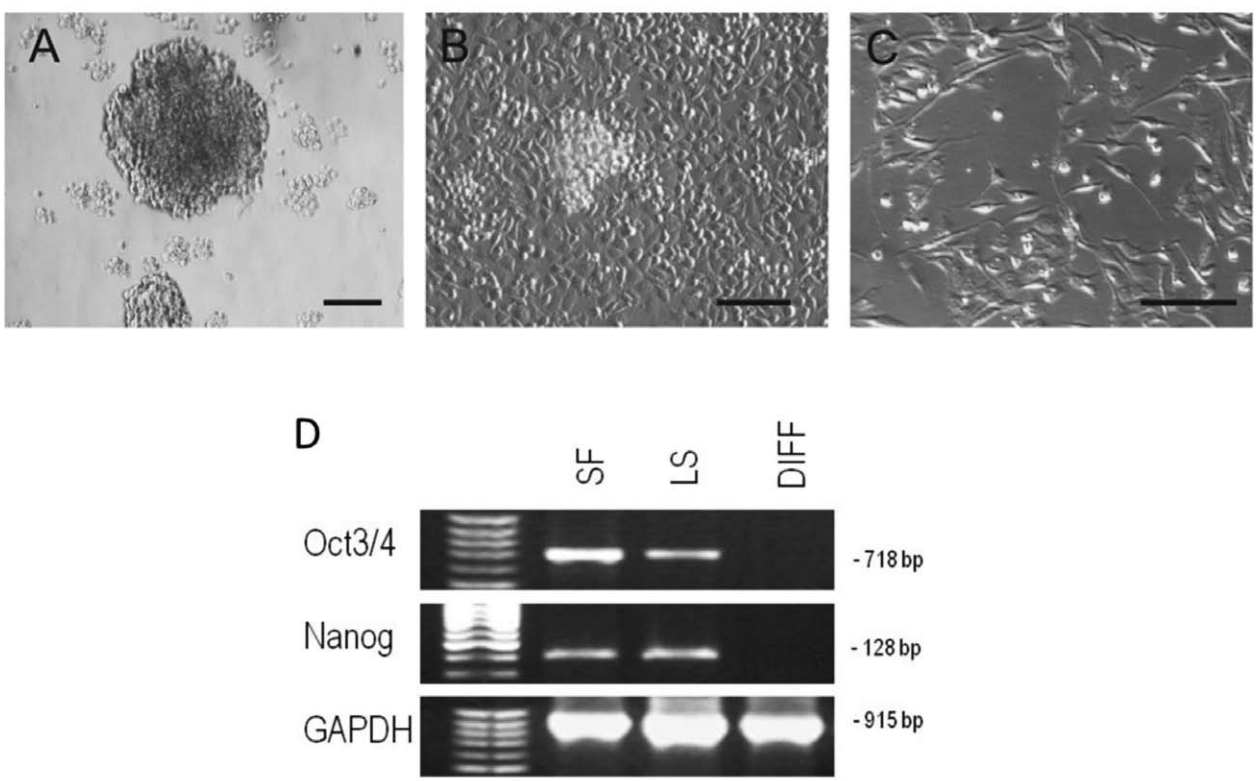

Fig. 1. Phase contrast image of HUCB-NSC from Serum-Free (A), Low Serum (B) and dBcAMP differentiation conditions (C). Scale bar 50 μm. Expression of Oct3/4 and Nanog gene in HUCB-NSC from serum-free (SF), low serum (LS) culture condition comparing to dBcAMP differentiated cells (DIFF). GAPDH gene is used as housekeeping gene (D).

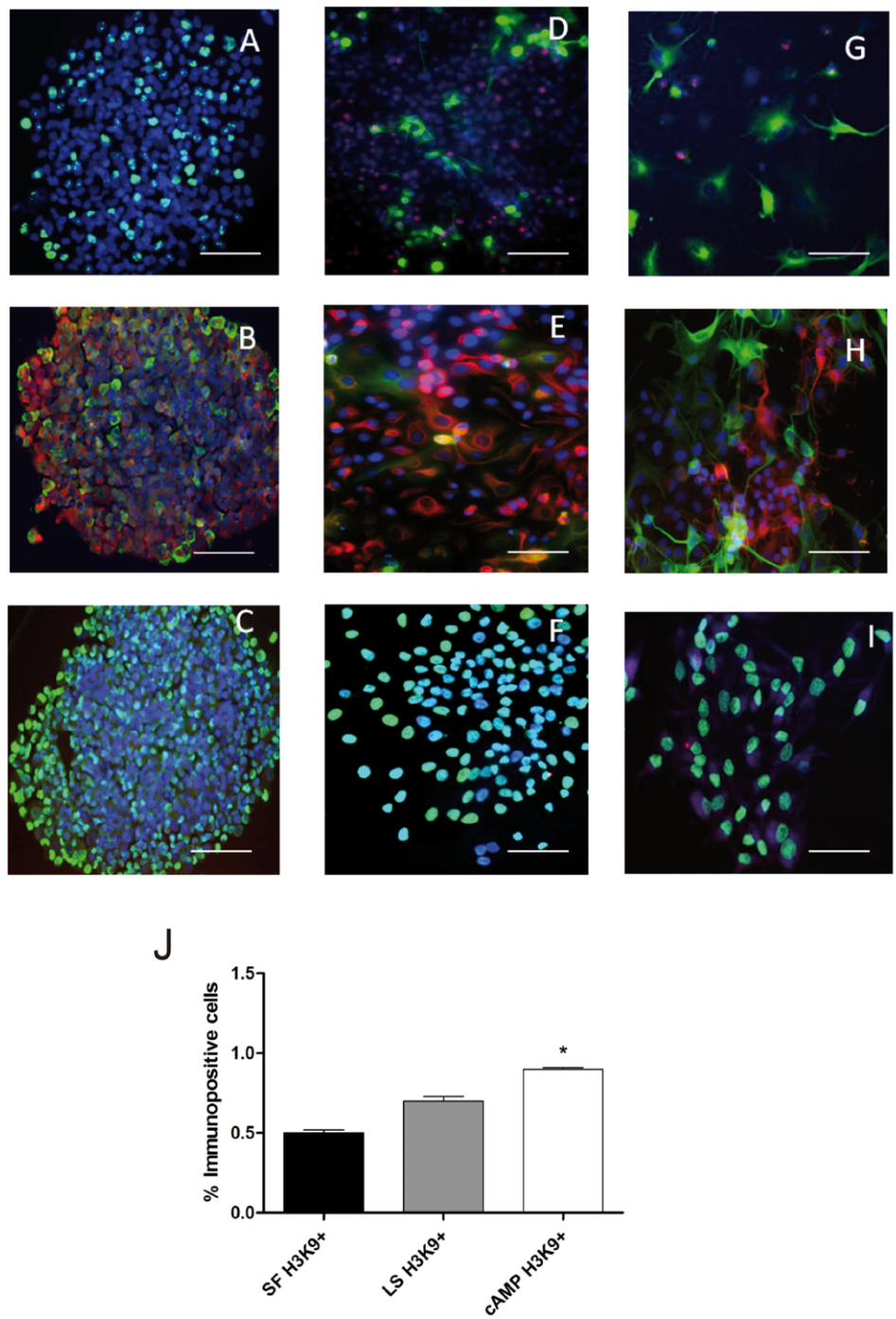

Fig. 2. Immunostaining of HUCB-NSCs under serum free (SF), low serum (LS) and dBcAMP differentiating culture conditions (DIFF) in vitro. Cells from SF cultures conditions expressing Ki67 (green) (A), Nestin (green) and GFAP (red) (B), H3K9me3 (green) (C). Cells cultured in low serum medium expressing Ki67 (red) and class III beta-tubulin (green) (D), NF200 (red) and class III beta-tubulin (green) (E), H3K9me3 (green) (F). Cells treated with dBcAMP expressing Ki67 (red) and class III beta-tubulin (green) (G), MAP2 (red) and class III beta-tubulin (green) (H), H3K9me3 (green) (I). Cells nuclei were stained with Hoechst 33252 (blue). Scale bars are 50 µm. The bottom: frequency analysis of H3K9me3 expression in HUCB-NSC from serum free, low serum and cAMP differentiating culture conditions. Results are expressed as the mean ± SD of percent of positive cell nuclei in total cell number from three independent cultures. *P<0.05(J).

free medium (SF), the HUCB-NSCs grew as neurosphere-like aggregates or free floating undifferentiated cells (Figs 1A and 2) positive for nestin (69.1 ± 1.1%) and GFAP (84.1 ± 4.4%), Morphologically they resemble primitive neural phenotypes characteristic of the stem cells residing in CNS niches (Doetsch 2003). The next stage of NSC development in culture was attained in media containing relative low serum concentration (LS). Here the culture was grown as a mixture of undifferentiated, non-attached, round cells or already adherent, spindle-shaped cells. Among adherent cells we found these expressing early neural differentiation markers such as nestin, GFAP or NF200 (Figs 1B and 2) but never cells presenting more advanced neuronal markers. After neuromorphogenic stimulation by dBcAMP addition (Fig. 1C and 2) these cells differentiated toward heavily branched, non-dividing terminally differentiated neurons expressing characteristic proteins like dendrite-localized MAP2 (39 ± 1.6%) (Fig. 2H).

All described above steps of HUCB-NSC neuronal differentiation coincided with alteration of Oct3/4 and Nanog STF gene expression (Fig. 1D) progressively silenced up to complete inhibition in the dBcAMP-treated cells.

DNA methylation profiles of Oct3/4 and Nanog genes upon neural differentiation of HUCB-NSC

The DNA methylation pattern of two stem-cell-marker (STM) genes, Oct3/4 and Nanog, were analyzed in their enhancer and promoter regions by the bisulfite sequencing method to establish modifications in cytosine methylation profiles in CpG pairs upon neuronal differentiation. The reference probes of DNA methylation were performed on the human hESC DNA respectively.

Oct3/4 methylation

The distal enhancer (DE) of Oct3/4 promoter has been sequenced in the region between −2609 to −2362 nucleotides in relation to the transcription starting site (TSS) and covered four CpG pairs (Fig. 3). In the case of Nanog, the promoter was divided into 3 amplicons which collectively covered 14 5'-3' CpG pairs within the region of −1503 to −163 nucleotides from TSS site (Fig. 3, and Table I showing the bisulfate sequencing primers [BiS]).

The bisulfite sequencing of the DE region in Oct3/4 gene of referenced hESCs revealed that not more than 10% of examined CpG pairs is methylated (Fig. 4A). This level was similar to previously reported Oct3/4 methylation status of undifferentiated embryonic carcinoma cell line, NT2 (Deb-Rinker et at. 2005) and human ESC (Yeo et al. 2007). Comparing to these ESC probes, the undifferentiated neural stem cells derived from human umbilical cord blood and kept in serum-free culture conditions revealed much higher CpG methylation with 45% frequencies in the Oct3/4 gene DE promoter region (Fig. 4). Upon serum introduction and in parallel with the next, more advanced (LS) step of HUCB-NSC differentiation, these *cis* elements of Oct3/4 gene promoter became substantially more methylated, reaching about 70% frequencies. However, this increase in our experiments did not attaine statistical significance *(P*=0.31). Consistently with this observation, the transcriptional activity of Oct3/4 gene in cells grown in serum-free (SF) and low-serum (LS) media did not differ significantly when assayed by real-time qPCR (Fig. 5).

Analysis of differentiated HUCB-NSC cultures after dBcAMP treatment revealed further Oct3/4 DNA hypermethylation with frequency up to 95% of examined CpG islands ($P<0.05$; Fig. 4A). Accordingly, the dBcAMP treated HUCB-NSCs attained mature neuronal phenotypes with well branched cells highly immunopositive for class III beta-tubulin (43.5 ± 3.5%) and MAP2 neuronal markers (39 ± 1.6%) (Fig. 2H).

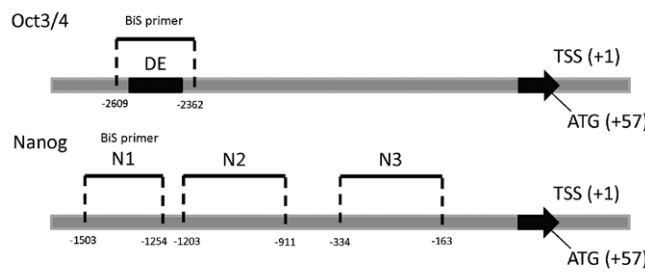

Fig. 3. OCT3/4 and NANOG promoter regions examined by bisulfite sequencing in this study. Localization of amplicons generated with BiS primers is shown. The nucleotide numbers are given in relation to the transcription start site (TSS; 1). (DE) distal enhancer.

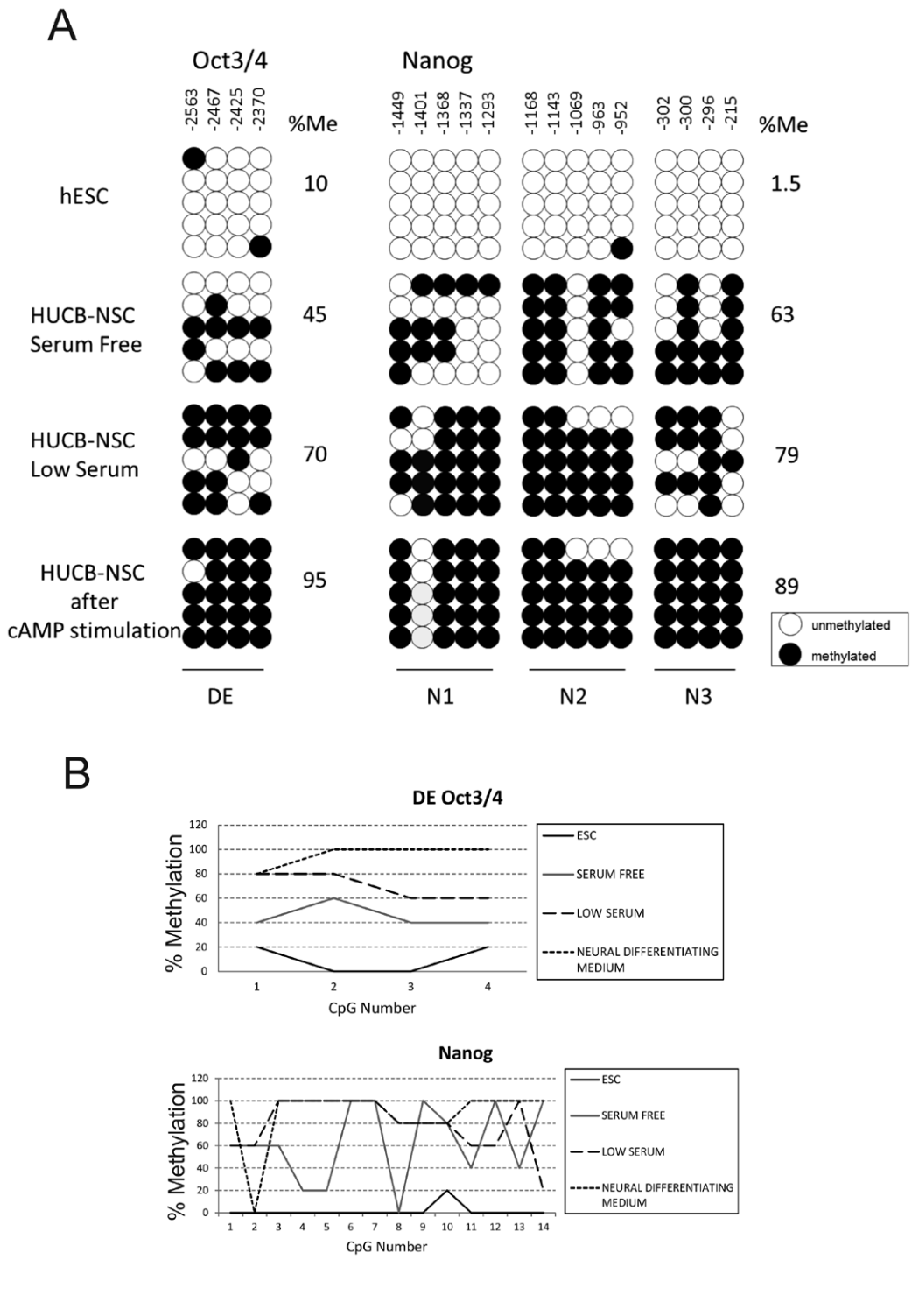

Fig. 4. Bisulfite sequencing analysis of Oct3/4 and Nanog methylation in hESC, HUCB-NSC from serum- free conditions, HUCB-NSC from low serum conditions and HUCB-NSC differentiated toward neuronal lineages. Top numbers indicate CpG number relative to the TSS. Global percentages of methylated cytosines (%Me) are shown. Each row of circles for a given amplicon represents the methylation status of each CpG in one bacterial clone for that region. Series of 5 clones are shown (A). Percentages of methylated cytosines in each position in Oct3/4 and Nanog determined from data shown in A (B).

Nanog methylation

Next we have assessed DNA methylation in the promoter region of Nanog gene. Three regions described above (Fig. 3) were selected. In the reference analysis of hESCs these regions revealed almost complete lack (1.5% of frequencies) of the examined cytosine methylation. In contrast, undifferentiated HUCB-NSC cells growing under serum-free conditions displayed as high as 63% of cytosine methylation frequency in all examined CpG pairs. The N1 fragment containing 5 first CpG pairs (−1449 to −1293) was less methylated comparing to N2 and N3 fragments (Fig. 4A). Introduction of serum into LS cultures led to further but non significant increase in this cytosine-CpG methylation in Nanog promoter to relative high level of 79% (Fig. 4A). As mentioned before and despite of the substantial increase in DNA methylation, the parallel analysis of Nanog transcriptional activity revealed similar level of mRNA in both, SF and LS culture conditions (Figs 1D and 5).

Under treatment with dBcAMP expression of Nanog mRNA declined rapidly together with further and significant increase of examined cytosine CpG pairs methylation in the Nanog promoter up to 89% (P<0.008; Fig. 4A). Obtained profiles of these CpG methylation frequencies are represented graphically as their average cytosine methylation of a given CpG pairs on the bottom of Figure 4B.

Lack of changes in histone H3 modification on Oct3/4 and Nanog gene promoters in differentiating HUCB-NSC

According to recent data, phenotypic maturation and progressive silencing of SCM genes are linked, in addition to hypermethylation of the DNA CpG, to significant post translational modification (PTM) of the genomic histone H3 structure. As shown on Figure 5 our analysis included three modifications associated with transcriptionally active genes (Pol2-CTD, H3Ac and H3K4me3) then two others associated with repressed genes (H3K9me3 and H3K27me3). Unexpectedly and in contrast to observed Oct3/4 and Nanog promoters DNA hypermethylation, the ChIP analysis did not reveal any significant changes in histone H3 PTM in regulatory regions of investigated STF gene promoters with only exception of Pol2-CTD slightly down-regulated upon differentiation. Interestingly, in the case of repressive H3K9met3 and H3K27met3 modifications, the PTMs remained stable even in constitutively active (ACTB) or permanently silenced (RHO) marker genes (Fig. 5). In contrast, activating modifi-

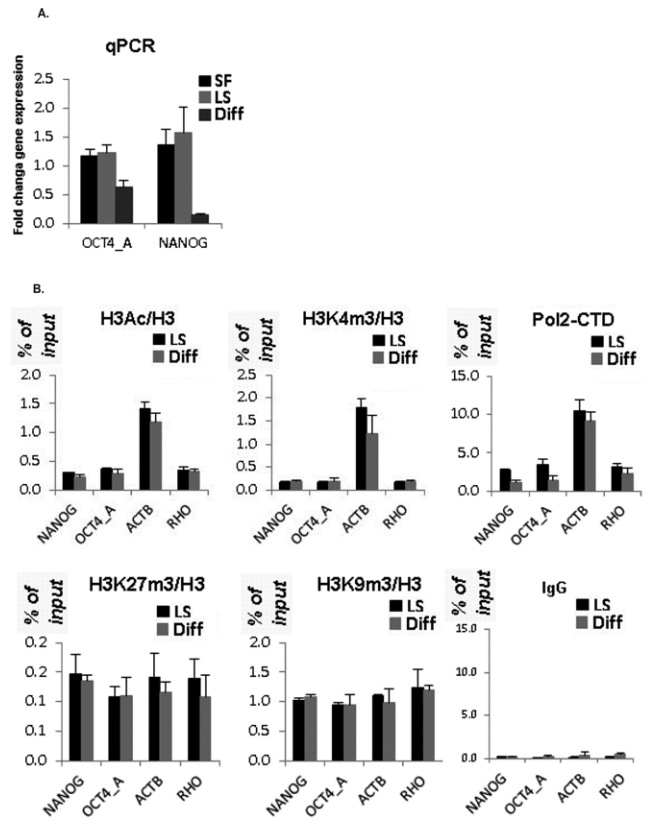

Fig. 5. (A) Quantification of transcriptional activity of Oct3/4 and Nanog genes at defined stages of HUCB-NSC differentiation. (B) Histone H3 Methylation and Acetylation Profiles in cultures demonstrating high (LS) and low (cAMP) levels of Oct3/4 and Nanog gene transcriptional activities: Histone H3 lysine K9/K18 acetylation (H3Ac) and Histone H3 lysine K4 methylation (H3 K4me3), the markers of transcriptionally active chromatin, remained unchanged along promoters of STF genes, resembling levels present on RHO (constitutively silenced) marker gene promoter. The levels of polymerase 2 (Pol2-CTD) revealed slight, but statistically non-significant decline associated with developmentally regulated gene expression. The ACTB and RHO promoters showed high and low levels of these activating PTMs, what reflects well transcriptional activity characteristic for these cells. Histone H3 methylation on lysine K9 (H3K9me3) and on lysine K27 (H3K27me3), the markers of repressive chromatin state, remain unchanged in investigated here different states of gene expression including also the lack of typical response from promoters of highly transcribed (ACTB) or constitutively silenced (RHO) marker genes.

cations of H3K4me3, H3Ac stayed also unchanged but on relatively low levels, similar to that characteristic for constitutive silent RHO marker gene, whereas in constitutively transcribed ACTB gene these PTMs were significantly enhanced (Fig. 5).

Enhanced overall Histone H3 lysine K9 trimethylation (H3K9me3) in differentiating HUCB- NSC

The post translational modifications of the amino-terminal tails of the H3 histone also involve general changes in condensation of chromatin connected with various STF regulatory and differentiation-specific genes, which maintain them in either an activated or repressed state. The gene repression and chromatin condensation by H3 histone trimethylations on lysine 9 (H3K9me3) or the transcriptional activation through the trimethylation of lysine 4 (H3K4me3) are the approved markers of these general processes. Therefore, in the next experiments, HUCB-NS cells were tested for the overall expression of both H3K4me3 and H3K9me3 chromatin modification markers in cell nuclei of HUCB-NS cells. Western blot analysis with histone H3 antibodies revealed a much higher concentration of the repressive H3K9me3 heterochromatin marker than the transcriptionally permissive H3K4me3 marker in the neural committed albeit still proliferating LS cultures (Fig. 6A). This finding, further confirmed by cell immunocytochemistry, revealed a significantly higher frequency of H3K9me3 immunopositive cell nuclei over that of H3K4me3 reactive nuclei in parallels performed mono- (Fig. 6A) as well as double-labeling experiments (Fig. 6B). This observation is in line with the general notion about the preferential role of the gene silencing over transcription permissive PTMs during cell differentiation (Maherali et al. 2007).

We tested the relations between these repressive

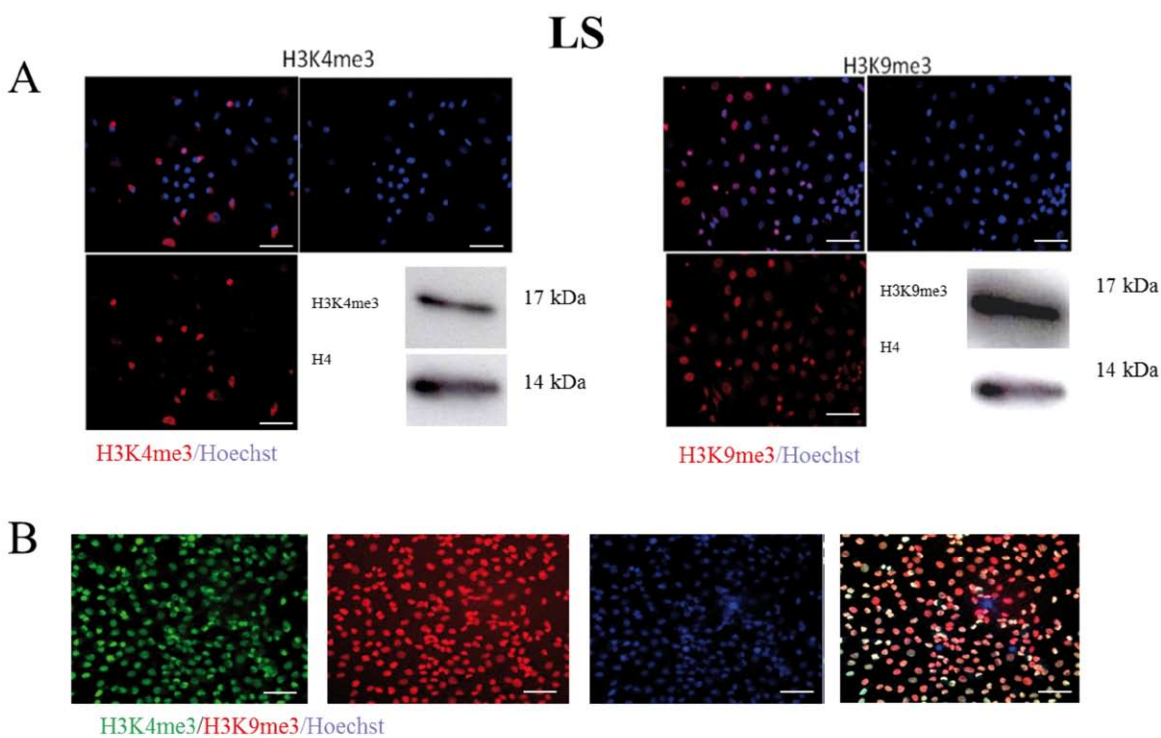

Fig. 6. Chromatin condensation marks in HUCB-NS cells differentiation. (A) Immunocytochemistry (red staining) and Western Blots for the euchromatin marker H3K4me3 (left side) and the transcriptional repressor marker H3K9me3 (right side) in HUCB-NSC culture growing under low serum (LS) conditions. The input blot with histone H4 is shown twice with H3K4me3 and H3K9me3 WB presentation. Scale bars are 20 µm, Hoechst 33252 (blue) for total cell nuclei label (A). Immunofluorescent H3K4me3 labeling (green) and H3K9me3 labeling (red) in low serum (LS) HUCB-NSC cultures. Scale bars are 20 µm, Hoechst 33252 (blue) for total cell nuclei label (B).

histone H3K9me3 modifications and the steps of HUCB-NSC maturation. We have found a progressive and significant increase of the number of H3K9me3 positive cell nuclei (Fig. 2) when comparing undifferentiated serum-free (SF 49.8 ± 3.1%), low-serum (LS 67.5 ± 4.6%) and terminally differentiated cultures, respectively (96.6 ± 0.6%). Immunocytochemistry also revealed that H3K9me3 reactivity at the early stage of cell differentiation were located almost exclusively in the most peripheral welt around of neurosphere-like cell aggregates with their center remaining free of this repressive nuclear marker (Fig. 2C). The similar distribution of other neural differentiation immunomarkers was noticed previously in CB cell aggregates (Habich and Domanska-Janik 2011) and further confirmed here (Fig. 2B) by the labeling with Nestin as one of the most primitive neuroectodermal marker. In this case nestin immunopositive cells are located mainly in center of neurosphere on Figure 2B. In contrast, GFAP immunoreaction, being characteristic for differentiating glial cells, is situated on periphery of aggregate. Thus, the H3K9me3 antibody seems to sharply discriminate between the subtle but distinct subsets of cells in proliferating neural progenitor fraction (see evenly distributed proliferating cell marker Ki67 in the same aggregate at Fig. 2A) attaining different stages of development and chromatin condensation. In light of this finding H3k9me3 expression could serve as a sensitive marker to label the cells approaching the path of early neural commitment (nestin$^{+/}$GFAP^{+}/ H3K9me3^{+}) in contrast to more primitive, undifferentiated progenitors (nestin^{+}/GFAP^{-}/H3K9me3^{-}) residing in stem cell niche. Under culturing in the LS condition or dBcAMP induced differentiation HUCB-NSC expressed successively increasing number of nuclei reacting positively with H3-histone-K9me3 antibody which follow successive changes toward maturated neuronal cell phenotypes (Fig. 2G, H, I).

DISCUSSION

The susceptibility of immature cord blood-derived cells to dedifferentiation and reprogramming is often linked with the specific ("open") epigenetic status of their transcriptosome. It concerns mainly a small subset of typical STF genes being actively transcribed in CB mononuclear fraction (McGuckin et al. 2005, Habich and Domanska-Janik 2011). The cord blood NSC line investigated in this work was shown previously (Buzanska et al. 2002, 2009) to display a substantially high inherited plastic capacity, enabling the cells to attain precise stages of sequential neural commitment and maturation *in vitro*. However, this raises the question as to the extent of which specific epigenetic marks or correlates of the overall chromatin organization help to better understand this unique behavior of HUCB-NSC culture. Our results have shown that multipotent, undifferentiated cells growing in serum-free (SF) conditions or in cultures promoting an early stage of neural commitment in the low-serum (LS) expansion media, express similar, relatively high level of the leading SCM genes such as Oct3/4 and Nanog transcriptional activity (Figs 1D and 5). This observation is in accordance with previously reported data, that demonstrates the expression of pluripotency genes in the native as well as neurally directed cord blood fractions (McGuckin et al. 2005, Habich et al. 2006, Kucia et al. 2007). However in spite of high STF genes expression in both SF and LF fractions, we have noticed substantial levels of repressive DNA methylation (45% and 67% in the cases of Oct3/4 and Nanog, respectively).

Finally, only when the cells were cultivated for a suitably long period in dBcAMP medium to acquire mature neuronal phenotypes, they did exhibit an almost completed DNA methylation of the investigated SCM gene promoters (up to 90–95% of examined CpG pairs) linked with genes silencing. Transcriptionally silencing PTM observed evenly on early stages of HUCB-NSC development, suggests that expression of these two pluripotency marker genes can be either inhibited exclusively by very specific DNA methylation pattern or that certain loci of cytosine methylation are more decisive for these genes silencing than others. Based on our current knowledge, it is not possible to conclude if the observed inconsistency between substantial methylation in the promoter regions of transcriptionally active Oct3/4 and Nanog genes is due to cell population heterogeneity or whether this imposition reflects a certain level of "silent" hits on transcriptionally inactive gene loci. However, in this context it should be mentioned that the expression of STF genes in cord blood was found to be evenly distributed rather than limited to the distinct cell subsets with unique, ESCs- like transcriptosomal characteristic (Giorgetti et al. 2010).

Nonetheless, the final down-regulation of Oct3/4 and Nanog upon advanced HUCB-NSC differentiation is evidently linked with further, almost complete cytosine methylation (up to 90–95% of examined CpG pairs) demonstrated here on STF gene promoters. This observation further supports the theory that cell differentiation is governed to certain extent, by very specific DNA methylation sites on SCM gene promoters resulting in the silencing of these genes. A similar conclusion was derived from the observation that different levels of DNA and histone H3K9 methylation on the Oct3/4 promoter region accompany this gene repression in differentiating mouse ESC (Lee et al. 2004). But in view of the substantial cytosine CpG methylation without relevant genes repression in SF and LS cultures, we also have to conclude that the simple imposition of methylation in the promoter region is probably not an executive trigger for these genes repression. A second important characteristic currently linked with differentiation/dedifferentiation and cell nuclear reprogramming is an actual status of histone post translational modification (PTM). The majority of genes in ESC and all active genes in differentiated cells stay preferentially in an uncondensed configuration. This coincides with relatively high level of methylated histone H3 on lysine 4 (H3K4 me3) and with low content of the histone H3 methylated lysine 9 (H3K9me3) on these gene specific promoter regions (Armstrong et al. 2006).

Accordingly, our data revealed that the expression of both, K4 and K9-connected H3 histone PTM markers in cell nuclei of expanding HUCB-NSC cultures showed a lower level of euchromatin marker H3K4me3 than the condensed heterochromatin marker H3K9me3 (Fig. 6). Moreover, the transcriptionally repressive lysine 9 methylation (H3K9me3) observed in 50% of the total cell nuclei number in undifferentiated (SF) cells, increased significantly to 67% in low serum and up to 97% upon dBcAMP induced terminal differentiation (Fig. 2). This finding is in line with concomitantly observed transcriptional repression of pluripotency associated SCM genes and almost complete methylation of DNA CpG pairs in their promoter regions. Mechanistically, methylated CpG elements can be recognized by methyl-CpG binding proteins that recruit histone deacetylase activity and thereby, in addition to lysine K9 methylation would induce also low acetylated state of inhibitory chromatin configuration. Moreover, the function of H3K9me3 is considered as a specific binding site for other various heterochromatin-specific proteins that can finely modulate nuclear chromatin organization (Stewart et al. 2005). In effect, this results in the inhibition and also the activation of a different set of genes.

CONCLUSIONS

In the present study, the positive correlation between: (1) methylation level of DNA CpG pairs in promoter regions of decisive genes encoding stemness transcriptional factors (STF) Oct3/4 and Nanog, (2) transcriptional repression of these selected STF genes, (3) the relatively high level of H3K9me3 repressive chromatin marker expression in cell nuclei, (4) stage differentiation of HUCB-NSC has been found. These findings agree with other studies, indicating that nuclear chromatin reorganization plays an important role during terminal differentiation of neural progenitors (Prasad et al. 2012).

However, in contrast to the aforementioned interrelation between the overall changes in H3-histone methylation pattern and examined CpG cytosine methylation status at DNA promoters upon HUCB-NSC differentiation, the performed ChIP analysis did not reveal any conclusive, maturation-specific PTM changes in the selected Oct3/4 and Nanog gene promoters (Fig. 5). Indirectly, this finding may suggest that the observed repression of the stemness-connected transcription factors in correlation with HUCB-NSC differentiation relays mainly, if not exclusively, on DNA CpG modifications. However, the data obtained does not allow us to answer if this behavior is an inherited attribute of cord blood cell plasticity or if this stiffness of the main STF genes to epigenetic histone PTM is linked with aberrant chromatin modification acquired during long term HUCB-NSC culturing.

ACKNOWLEDGMENTS

This work was sponsored by National Science Center, grant no 0141/P01/2008/35, 05401/B/ NZ3/2011/01, and 5978/B/P01/2010/38. We are cordially grateful to Prof P. Dvorak for his generous gift with hESC DNA probes. We also want to thank Jerzy Ostrowski and Michal Mikula for technical support with Matrix ChIP and assistance in statistical analysis.

REFERENCES

Ali H, Jurga M, Kurgonaite K, Forraz N, McGuckin C (2009) Defined serum-free culturing conditions for neural tissue engineering of human cord blood stem cells. Acta Neurobiol Exp (Wars) 69: 12–23.

Armstrong L, Lako M, DeanW, Stojkovic M (2006) Epigenetic modification is central to genome reprogramming in somatic cell nuclear transfer. Stem Cell 24: 805–814.

Bonner-Weir S, Inada A, Yatoh S, Li WC, Aye T, Toschi E, Sharma A (2008) Transdifferentiation of pancreatic ductal cells to endocrine beta-cells. Biochem Soc Trans 36: 353–356.

Borowiak M, Melton DA (2009) How to make beta cells? Curr Opin Cell Biol 21: 727–732.

Buzańska L, Machaj EK, Zabłocka B, Pojda Z, Domańska-Janik K (2002) Human cord blood-derived cells attain neuronal and glial features in vitro. J Cell Sci 115: 2131–2138.

Buzańska L, Jurga M, Stachowiak EK, Stachowiak MK, Domańska-Janik K (2006) Neural stem-like cell line derived from a nonhematopoietic population of human umbilical cord blood. Stem Cells Dev 15: 391–406.

Buzanska L, Sypecka J, Nerini-Molteni S, Compagnoni A, Hogberg HT, del Torchio R, Domanska-Janik K, Zimmer J, Coecke S (2009) A human stem cell-based model for identifying adverse effects of organic and inorganic chemicals on the developing nervous system. Stem Cells 27: 2591–2601.

Chua SJ, Bielecki R, Wong CJ, Yamanaka N, Rogers IM, Casper RF (2009) Neural progenitors, neurons and oligodendrocytes from human umbilical cord blood cells in a serum-free, feeder-free cell culture. Biochem Biophys Res Commun 379: 217–221.

Deb-Rinker P, Ly D, Jezierski A, Sikorska M, Walker PR (2005) Sequential DNA methylation of the Nanog and Oct-4 upstream regions in human NT2 cells during neuronal differentiation. J Biol Chem 280: 6257–6560.

Doetsch F (2003) A niche for adult neural stem cells. Curr Opin Genet Dev 13: 543–550.

Domanska-Janik K, Buzanska L, Lukomska B (2008) A novel, neural potential of non-hematopoietic human umbilical cord blood stem cells. Int J Dev Biol 52: 237–248.

Flanagin S, Nelson JD, Castner DG, Denisenko O, Bomsztyk K (2008) Microplate based chromatin immunoprecipitation method, Matrix ChIP: a platform to study signaling of complex genomic events. Nucleic Acids Res 36 (3): e17.

Freberg CT, Dahl JA, Timoskainen S, Collas P (2007) Epigenetic reprogramming of OCT4 and NANOG regulatory regions by embryonal carcinoma cell extract. Mol Biol Cell 18: 1543–1553.

Giorgetti A, Montserrat N, Rodriguez-Piza I, Azqueta C, Veiga A, Izpisúa Belmonte JC (2010) Generation of induced pluripotent stem cells from human cord blood cells with only two factors: Oct4 and Sox2. Nat Protoc 5: 811–820.

Haase A, Olmer R, Schwanke K, Wunderlich S, Merkert S, Hess C, Zweigerdt R, Gruh I, Meyer J, Wagner S, Maier LS, Han DW, Glage S, Miller K, Fischer P, Schöler HR, Martin U (2009) Generation of induced pluripotent stem cells from human cord blood. Cell Stem Cell 5: 434–441.

Habich A, Jurga M, Markiewicz I, Lukomska B, Bany-Laszewicz U, Domanska-Janik K (2006) Early appearance of stem/progenitor cells with neural-like characteristics in human cord blood mononuclear fraction cultured in vitro. Exp Hematol 34: 914–925.

Habich A, Domanska-Janik K (2011) Aggregation-promoted expansion of neurally committed human umbilical cord blood progenitors in vitro. Acta Neurobiol Exp (Wars) 71: 1–11.

Jurga M, Lipkowski AW, Lukomska B, Buzanska L, Kurzepa K, Sobanski T, Habich A, Coecke S, Gajkowska B, Domanska-Janik K (2009) Generation of functional neural artificial tissue from human umbilical cord blood stem cells. Tissue Eng Part C Methods 15: 365–372.

Kögler G, Sensken S, Airey JA, Trapp T, Müschen M, Feldhahn N, Liedtke S, Sorg RV, Fischer J, Rosenbaum C, Greschat S, Knipper A, Bender J, Degistirici O, Gao J, Caplan AI, Colletti EJ, Almeida-Porada G, Müller HW, Zanjani E, Wernet P (2004) A new human somatic stem cell from placental cord blood with intrinsic pluripotent differentiation potential. J Exp Med 200: 123–135.

Kucia M, Halasa M, Wysoczynski M, Baskiewicz-Masiuk M, Moldenhawer S, Zuba-Surma E, Czajka R, Wojakowski W, Machalinski B, Ratajczak MZ (2007) Morphological and molecular characterization of novel population of CXCR4+ SSEA-4+ Oct-4+ very small embryonic-like cells purified from human cord blood: preliminary report. Leukemia 21: 297–303.

Lee JH, Hart RS, Skalnik DG (2004) Histone deacylase activity is required for embryonic stem cell differentiation. Genesis 38: 32–38.

Lee MW, Moon YJ, Yang MS, Kim SK, Jang IK, Eom YW, Park JS, Kim HC, Song KY, Park SC, Lim HS, Kim YJ

(2007) Neural differentiation of novel multipotent progenitor cells from cryopreserved human umbilical cord blood. Biochem Biophys Res Commun 358: 637–643.

Maherali N, Sridharan R, Xie W, Utikal J, Eminli S, Arnold K, Stadtfeld M, Yachechko R, Tchieu J, Jaenisch R, Plath K, Hochedlinger K (2007) Directly reprogrammed fibroblasts show global epigenetic remodeling and widespread tissue contribution. Cell Stem Cell 1: 55–70.

McGuckin CP, Forraz N, Allouard Q, Pettengell R (2004) Umbilical cord blood stem cells can expand hematopoietic and neuroglial progenitors in vitro. Exp Cell Res 295: 350–359.

McGuckin CP, Forraz N, Baradez MO, Navran S, Zhao J, Urban R, Tilton R, Denner L (2005) Production of stem cells with embryonic characteristics from human umbilical cord blood. Cell Prolif 38: 245–55.

Pfaffl MW (2001) A new mathematical model for relative quantification in real-time RT-PCR. Nucleic Acids Res 29: e45.

Prasad MS, Sauka-Spengler T, LaBonne C (2012) Induction of the neural crest state: control of stem cell attributes by gene regulatory, post-transcriptional and epigenetic interactions. Dev Biol 366: 10–21.

Reynolds BA, Rietze RL (2005) Neural stem cells and neurospheres--re-evaluating the relationship. Nat Methods 2: 333–336.

Sanchez-Ramos JR, Song S, Kamath SG, Zigova T, Willing A, Cardozo-Pelaez F, Stedeford T, Chopp M, Sanberg PR (2001) Expression of neural markers in human umbilical cord blood. Exp Neurol 171: 109–115.

Stewart MD, Li J, Wong J (2005) Relationship between histone 3 lysine 9 methylation, transcription repression and heterochromatine protein 1 recruitment. Mol Cell Biol 25: 2525–2538.

Sun W, Buzanska L, Domanska-Janik K, Salvi RJ, Stachowiak MK (2005) Voltage-sensitive and ligand-gated channels in differentiating neural stem-like cells derived from the nonhematopoietic fraction of human umbilical cord blood. Stem Cells 23: 931–945.

Vierbuchen T, Ostermeier A, Pang ZP, Kokubu Y, Südhof TC, Wernig M (2010) Direct conversion of fibroblasts to functional neurons by defined factors. Nature 463: 1035–1041.

Willing AE, Lixian J, Milliken M, Poulos S, Zigova T, Song S, Hart C, Sanchez-Ramos J, Sanberg PR (2003) Intravenous versus intrastriatal cord blood administration in a rodent model of stroke. J Neurosci Res 73: 296–307.

Yamanaka S (2007) Strategies and new developments in the generation of patient-specific pluripotent stem cells. Cell Stem Cell 1: 39–49.

Yeo S, Jeong S, Kim J, Han JS, Han YM, Kang YK (2007) Characterization of DNA methylation change in stem cell marker genes during differentiation of human embryonic stem cells. Biochem Biophys Res Commun 359: 536–542.

Yu J, Feng Q, Ruan Y, Komers R, Kiviat N, Bomsztyk K (2011) Microplate-based chromatin and DNA methylation immunoprecipitation assay. BMC Molecular Biology 12: 49.

Zaehres H, Kögler G, Arauzo-Bravo MJ, Bleidissel M, Santourlidis S, Weinhold S, Greber B, Kim JB, Buchheiser A, Liedtke S, Eilken HM, Graffmann N, Zhao X, Meyer J, Reinhardt P, Burr B, Waclawczyk S, Ortmeier C, Uhrberg M, Schöler HR, Cantz T, Wernet P (2010) Induction of pluripotency in human cord blood unrestricted somatic stem cells. Exp Hematol 38: 809–818.

Zigova T, Song S, Willing AE, Hudson JE, Newman MB, Saporta S, Sanchez-Ramos J, Sanberg PR (2002) Human umbilical cord blood cells express neural antigens after transplantation into the developing rat brain. Cell Transplant 11: 265–274.